E. Joffrin, F. Crisanti, R. Felton, X. Litaudon, D. Mazon, D. Moreau, L. Zabeo, R. Albanese,
M. Ariola, D. Alves, O. Barana, V. Basiuk, A. Bécoulet, M. Bécoulet, J. Blum,T. Bolzonnella,
K. Bosak, E. de la Luna, J.M. Chareau, M. de Baar, P. de Vries, P. Dumortier, D. Elbeze,
J. Farthing, H. Fernandes, C. Fenzi, R. Giannella, K. Guenther, J. Harling, N. Hawkes,
T. C. Hender, D. F. Howell, P. Heesterman, F. Imbeaux, P. Innocente, L. Laborde, G. Lloyd,
P. J. Lomas, D. C. McDonald, J. Mailloux, M. Mantsinen, A. Messiaen, A. Murari, J. Ongena,
F. Orsitto, V. Pericoli-Ridolfini, M. Riva, J. Sanchez, F. Sartori, O. Sauter, A. C. C. Sips,
T. Tala, A. Tuccillo, D. Van Ester, K.-D. Zastrow, M. Zerbini and JET EFDA contributors

Integrated Scenario in JET using Real Time Profile Control

Integrated Scenario in JET using Real Time Profile Control

E. Joffrin[1], F. Crisanti[2], R. Felton[3], X. Litaudon[1], D. Mazon[1], D. Moreau[1], L. Zabeo[1], R. Albanese[4], M. Ariola[5], D. Alves[6], O. Barana[7], V. Basiuk[1], , A. Bécoulet[1], M. Bécoulet[1], J. Blum[8],T. Bolzonnella[7], K. Bosak[8], E.de la Luna[12], J.M. Chareau[1], M. de Baar[9], P. de Vries[3], P. Dumortier[10], D. Elbeze[1], J. Farthing[3], H. Fernandes[6], C. Fenzi[1], R. Giannella[1], K. Guenther[3], J. Harling[3], N. Hawkes[3], T. C. Hender[3], D. F. Howell[3], P. Heesterman[3], F. Imbeaux[1], P. Innocente[7], L. Laborde[1], G. Lloyd[3], P. J. Lomas[3], D. C. McDonald[3], J. Mailloux[3], M. Mantsinen[11], A. Messiaen[10], A. Murari[7], J. Ongena[10], F. Orsitto[2], V. Pericoli-Ridolfini[2], M. Riva[2], J. Sanchez[12], F. Sartori[3], O. Sauter[13], A. C. C. Sips[14], T. Tala[15], A. Tuccillo[2], D. Van Ester[10], K.-D. Zastrow[3], M. Zerbini[2] and JET EFDA contributors*

[1]Association EURATOM–CEA, CEA/DSM/DRFC CEA-Cadarache, 13108 Saint Paul lez Durance, France.
[2]Associazione EURATOM-ENEA sulla Fusione, C.R. Frascati, Frascati , Italy.
[3]Euratom/UKAEA Fusion Association, Culham Science Centre, Abingdon, Oxon OX14 3DB, UK.
[4]Associazione EURATOM/ENEA/CREATE,DIS, Universita' di Napoli Federico II, Napoli, Italy
[5]Associazione EURATOM/ENEA/CREATE, DIMET, Universita' di Reggio Calabria, Italy
[6]Instituto Superior Técnico, Av. Rovisco Pais, 1049-001 Lisboa, Portugal
[7]Consorzio RFX - Associazione Euratom-Enea sulla Fusione, Corso Stati Uniti 4, I-35127 Padova.
[8]Universite de Nice-Sophia Antipolis, UMR 6621, Parc Valrose, 06108 Nice Cedex 02, France
[9]FOM-Rijnhuizen, Ass. Euratom-FOM, TEC, PO Box 1207, 3430 BE Nieuwegein, NL.
[10]Association Euratom-Belgian State, Royal Military Academy, Belgium.
[11]Association Euratom-Tekes, P.O.Box 2200, FIN-02015 HUT, Finland
[12]Associacion EURATOM-CIEMAT para Fusión, Avenida Complutense 22, E-28040 Madrid, Spain
[13]Association EURATOM-Confédération Suisse, EPFL, 1015 Lausanne, Switzerland
[14]IPP-EURATOM Assoziation, Boltzmann-Str.2, D-85748 Garching, Germany
[15]Association EURATOM-TEKES, VTT Processes, P.O. Box 1608, FIN-02044 VTT, Finland.
* See annex of J. Pamela et al, "Overview of Recent JET Results and Future Perspectives", Fusion Energy 2000 (Proc. 18th Int. Conf. Sorrento, 2000), IAEA, Vienna (2001).

ABSTRACT

The recent development of real time measurements and control tools in JET has enhanced the reliability and reproducibility of the relevant ITER scenarios. Diagnostics such as charge exchange, interfero-polarimetry, Electron Cyclotron Emission (ECE) have been upgraded for real time measurements. In addition, real time processes like magnetic equilibrium and q profile reconstruction have been developed and applied successfully in real time q profile control experiments using model based control techniques. Plasma operation and control against MHD instabilities are also benefiting from these new systems. The experience gained at JET in the field of real time measurement and control experiments operation constitutes a very useful basis for the future operation of ITER scenarios.

INTRODUCTION

In recent years, the preparation of ITER scenarios [1, 2] has been the main focus of tokamaks experimental activity and operation. As the studies progress, the development and operation of these scenarios demand the integration of increasing numbers of control parameters. The development of systems for the active control of plasma shape, current and pressure profiles [3], radiation [4], Magneto-Hydro-Dynamic (MHD) instabilities, etc… is now the most outstanding issue for burning plasma operation on ITER. Experiments with the real time control of Internal Transport Barriers (ITB) [5], MHD instabilities [6, 7] and current profile [8] have already produced promising results in various large devices such as DIII-D, JT-60, and Tore Supra.

In this context, JET has developed since 2001 a comprehensive set of real time diagnostics, control tools and simulation facilities for the operation of the reference ITER scenario and advanced tokamak scenarios. This enhancement project, undertaken under the European Development Fusion Agreement (EFDA), is now playing a decisive role in the operation of the JET device. In particular, the reliability and stability of ITER relevant plasma scenarios in JET have been improved and stability thanks to the use of the real time control tools [9, 10, 11]. Among the recent tools developed in JET, the real time equilibrium solver, together with real time electron and ion temperature and current profile measurements, has dramatically enhanced the experimental work on the integration of advanced tokamak scenarios and in particular the development of the techniques to control the q and pressure profiles simultaneously in real time [12].

This paper reports the technical and scientific achievements made in JET in this domain. The development of the new real time tools and algorithms are first described with respect to their relevance to real time control experiments. Practical examples in relevant ITER scenarios are given and the methodology used in JET to prepare and execute real time profile control experiments for the advanced tokamak scenarios are highlighted along with the modelling activity for these experiments. Finally, the benefits of real time control for plasma safety (including disruption avoidance or plasma MHD instability control) and operation are also illustrated.

1. DEVELOPMENTS OF REAL TIME MEASUREMENTS AND CONTROL SYSTEMS IN JET

To achieve extended burn with a fusion gain Q close to 10 in stationary conditions, key physics issues [1] related to plasma performance need to be addressed. For the relevant plasma scenario, four physics issues can be identified:

- The control of confinement (or H factor) at sufficiently high density ($n \sim 0.85$ n_G) to produce the requisite fusion power and Q value. Depending on the scenario, this issue is closely related to the control of the q profile (see below in section 3)
- The control of the loss power and particle exhaust to ensure acceptable levels of helium (or ashes), plasma impurities and heat load on the divertor target. This also encompasses the control of ELMs to ensure adequate lifetime of the in-vessel components.
- The control of global Magneto-HydroDynamic (MHD) instabilities such as neo-classical tearing modes or Resistive Wall Modes (RWM) and the use of plasma control to reduce the effect of disruptions.
- The control of α-particles losses via collective instabilities to enable the transfer of α-particle energy to the thermal plasma.

In present day tokamaks, the last item can be partially investigated using, for example ion cyclotron resonance heating (ICRH) [13]. But it requires D-T operation to be fully tested. On the other hand, all the other issues must be addressed **together** to make the operational scenarios relevant to burning plasma operation. As a result, the active control of a plasma discharge will require the use of a wide range of real time sensor parameters and appropriate actuators.

Furthermore, the development of plasma operational scenario offering the prospect of establishing reactor relevant steady state operation has motivated the use of active profile control and has also increased the demands on the flexibility of plasma shaping, heating and current drive systems [14]. Although the detailed conditions for the creation of Internal Transport Barriers (ITBs) are still uncertain [15], the aim of these tools is to improve the stability and reliability of this mode of operation by the control of current and pressure profile simultaneously [12]. In real discharges, deviations from a reference scenario may indeed occur and increase with time if these profiles are not accurately controlled. For example, the diffusion of the current density profile is not uniform across the plasma cross-section. Local variations could trigger either plasma instabilities or the loss of the improved confinement regime. The feedback control of non-linearly linked parameters such as the q and pressure profile will therefore be needed.

For all these reasons, JET has developed in the last two years an ambitious enhancement programme of real time measurements and control tools (figure 1) with the ultimate aim of assisting the development of the ITER relevant scenario. A large number of key diagnostics have been upgraded to produce real time measurements routinely (Table I). Real time processes such as real time equilibrium and profile mapping have also been implemented (Table II). This was made possible by the recent improvements in diagnostic reliability and also, by the rapidly growing capabilities of computers and communication

networks. The upgrades were selected by their expected potential value to the scenario integration and the main experimental programme.

For the confinement parameters, the new fast calculation has been based on the JET flux boundary code XLOC [16] used for plasma shape control. Using magnetic and diamagnetic data it produces plasma parameters such as the diamagnetic energy (W_{dia}), internal inductance (li), and plasma separatrix geometry in less than 1ms [17, 18].

For the line integrated density the interferometer has been equipped with new fast ADCs (Analog Digital Converter) and a new fringe jump correction algorithm [19] has been installed and validated [20]. Together with the real time faraday rotation data from the far-infrared interferometer they are Abel-inverted in less than 10ms [21, 22] to infer the density and q profile using a plasma boundary geometry based on the XLOC data. To improve further the reconstruction of the current density profile, a new Grad-Shafranov solver [23] called EQUINOX [24] has been developed, validated and installed on JET and also in Tore Supra [25]. This new real time equilibrium code computes the magnetic equilibrium and density profiles in less than 10ms for each time step and the data is delivered every 20ms. Another version of this code includes internal flux measurements from the far-infrared polarimeter as input to compute the current density profile with more accuracy. The flux map built by the EQUINOX solver is also used to reconstruct the profile data such as density and electron and ion temperature onto the plasma flux grid.

To complement the real time measurement of the current profile, new fast ADCs have also been installed on the Motional Stark Effect (MSE) diagnostic [26] and the pitch angles are now produced in real time with a source rate of about 40samples per second. In the near future, this data will be processed in real time using the EQUINOX geometry to compute a q profile independently from the q profile inferred from polarimetric data [27].

For the electron and ion temperature and rotation real time profile, both the cyclotron emission radiometer [28, 29] and the charge exchange diagnostic [30] have also been upgraded and connected to the communication network. The latter is synchronised to the neutral beam and is processing the five-Gaussian spectral analysis in less than 50ms. These data are all re-mapped onto the flux grid from EQUINOX and the ITB criterion ρ^*_{Te} and ρ^*_{Ti} [31] are also inferred from this procedure for the control of the pressure profile during ITBs.

Other relevant data such as MHD magnetic signals, neutron signals, heavy impurity lines from X-ray and visible spectroscopy [32], and radiated power from bolometry are complementing this ensemble. In addition some specific processing such as ELM detection (using D_α signals), Z_{eff} and thermal energy calculations, have been included. All of these diagnostic data processing algorithms have been tested and validated on a large number of pulses to guarantee their robustness during the experiments. For example, the equilibrium code EQUINOX has been tested against EFIT on a database of more than 500 discharges with a large variety of magnetic configurations, plasma current and toroidal field strength.

All of the data produced as well as the data from the actuators (Neutral Beam injection, Lower

Hybrid wave, Ion Cyclotron Resonance Heating, gas and pellet fuelling) have been connected to an Asynchronous Transfer Mode (ATM) and Ethernet computer communication network (figure 1). They are available through a Real Time Signal Server (RTSS) and the experimental control algorithms are implemented in a Real Time Central Controller (RTCC) [33]. This unit is also being upgraded to facilitate the routine use of so-called Multi-Input Multi-Output (MIMO) control schemes which are required for current and pressure profile feedback control in particular.

2. REAL TIME CONTROL FEEDBACK EXPERIMENT FOR ITER SCENARIOS

In the last campaigns, JET has strengthened its programme on the validation of ITER scenarios. The real time control systems have played an increasing role in the integration and reliability of the scenarios relevant for the next step. In line with the ITER performance assessment [1], three different scenarios have been considered in JET as relevant for future ITER operation: a) the inductive ELMy H-mode scenario, b) the steady state scenario, and c) the so-called "hybrid" advanced tokamak scenario. The main characteristics of each of these scenarios are briefly described below, together with the feedback control scheme developed for each of them.

2.1. THE INDUCTIVE ELMY H-MODE SCENARIO

The inductive ELMy H-mode scenario in ITER [34] is aimed at producing $Q\sim10$ for a limited burn time of about 400s with $q<1$ in the plasma core. It will be performed with $q_{95}=3$, $\beta_N\sim1.8$, and $H_{98y}\sim1$ close to the Greenwald density (typically at $0.85\ n_G$) and would be conducted in ITER at high field (5.3T) and current (15MA) at a triangularity at the separatrix of about 0.48.

Figure 2 shows an ELMy H-mode inductive scenario where the radiation fraction has been feedback controlled by Argon injection for more than 5s. At constant input power, this scheme is equivalent to the control of the conducted and convected power on the target plates. The scenario has been performed with an ITER-like plasma configuration ($\delta=0.4$) at 90% of the Greenwald density and high frequency ($\sim$40Hz) type I ELMs. The confinement is not dramatically degraded by the impurity injection ($H_{89}=0.91$ and $\beta_N=1.5$). The feedback controller includes the filtering of the radiation fraction and uses both integral and derivative gains. After two seconds, the feedback controller stabilises the pulse to the requested value of 60% of the radiated power, which correspond to a loss power of 7MW and a deposited power of about 5-6MW/m^2 as deduced from the power footprint from infra-red camera measurements. In another experiment with this scenario [35] a second feedback loop has also been coupled to control the H factor with deuterium fuelling. This scenario has the potential to integrate simultaneous feedback control of the confinement and loss power and the ELM frequency to control the deposited power on the divertor target plates.

2.2. THE STEADY STATE SCENARIO.

In the steady state non-inductive ITER scenario at $Q\sim5$, the total current during current flat top phase is generated non-inductively by additional current drive and a dominant fraction of bootstrap current

4

(typically more than 50%). The q profile in the plasma core is non-monotonic and has a minimum between the q = 2 and q = 3 rational surface. In ITER, it would be performed with q_{95}=5 to 6, β_N~2.8, H_{98y}~1.6 and n/n_G~0.8. The plasma current would be 9MA to maximise the bootstrap current and, with the help of high confinement, to make this discharge steady state with Vloop~0.

Figure 3 shows a JET prototype of a steady state scenario [36] with real time control of the ion temperature gradient R/L_{Ti} with the neutral beam power. The target value of R/L_{Ti} has been set to 24 which, in JET, corresponds to a "non-stiff" profile [15]. The "no ITB" reference value is also indicated for comparison. This discharge uses lower hybrid current drive (LHCD) to sustain the reversed q profile after it has been pre-formed in the early phase before 4s. At this time a wide ITB (R~3.6m) is created as q_{min} reaches the q = 3 surface [37]. A second, more internal, ITB (R~3.3m) is also present. Real time control of R/L_{Ti} assists the maintenance of the outer ITB until the end of the pulse using a proportional-integral controller. The electron temperature profile also shows a very steady electron ITB as illustrated by the ρ^*_{Te} criterion [31] in figure 3. The modest strength of these ITBs (ρ^*_{Te} ~0.02) is probably preventing the accumulation of impurities in the plasma core during this discharge as revealed by the impurity analysis [36]. Although this regime is operated at low density (n/n_G=0.4) and is not fully non-inductive (V_{loop} = 50mV, with 35% LH-current, 35% bootstrap current and ~15% NB-current), it provides an adequate target for implementing the control of the q profile together with the pressure profile up to the technical limit at JET(~20s).

2.3 THE "HYBRID" ADVANCED TOKAMAK SCENARIO

In this more recent mode of operation, current drive power and bootstrap current drive a substantial fraction of the total current. The burn time in ITER would, therefore, be significantly increased with respect to the inductive scenario to about 1000s. For this regime, the core q profile lies between 1 and 1.5 with a magnetic shear close to 0. In ITER, this scenario would be operated with q_{95} = 4, β_N ~2.8 and H_{98y} ~1.5 and n/n_G = 0.8 with a plasma current of 12MA.

The hybrid scenario has been achieved recently in JET in an experiment attempting to produce identity and similarity experiments with ASDEX-Upgrade [38]. Figure 4 presents an example of the hybrid scenario produced in JET [39] using the feedback control of the normalised beta β_N with the neutral beam power. The requested β_N waveform has two plateaux at β_N=2 and β_N=2.8 with the aim being to test the confinement behaviour as the power increases. In this scenario, only low amplitude 3/2 and 4/3 NTM modes (both with island size of the order of 3cm) are observable during the whole discharge, neither of which have a major deleterious effect on the confinement [40]. This feedback control scheme is very relevant to this regime since the β_N real time control could be used for preventing the growth of NTMs when they are approaching their β_N limit. In this scenario, the q profile is close to q = 1 in the plasma core as shown by the regular n = 1 m = 1 fishbone activity throughout the discharge. The ELMs are type I, but with high frequency (~30Hz). The ELM frequency increases slightly during the second power phase. The non-inductive current fraction of this discharge is around 46% shared equally between bootstrap and beam driven current. This discharge reached only 50% of

the Greenwald density in a low triangularity configuration (δ~0.2). However, similar experiments, 85% of the Greenwald density has been achieved using an ITER-like shape configuration with δ=0.45 [39]. The real time control of the q profile and of NTMs at high normalised beta and high triangularity are therefore amongst the most favoured control schemes considered for future experiments.

The new real time systems developed at JET have started to contribute to the integration of ITER scenarios. As a result, the reliability of these scenarios has been improved significantly. However, these experiments are limited to a simple real time network using the control of one output by one actuator. In particular for the steady state scenario, they have also revealed the need for the feedback control of profiles, which requires the use of several controlled outputs by several actuators (multi-input multi-output). Within the real time project, JET has started to develop the control techniques and the necessary algorithms for achieving this goal; this is described in the next section.

3. FEEDBACK EXPERIMENT USING REAL TIME PROFILE CONTROL
3.1 DESIGN OF A REAL TIME CONTROLLER FOR TOKAMAK

For the design of multi-input multi-output controller for real time profile control, let us first consider the layout of a general control system for a tokamak as presented in figure 5. For simplicity, all the transfer functions are linearised and represented by their Laplace transforms. This layout can be mainly divided into two blocks: the plant and the controller. In the plant, the plasma transfer function $K(s)$ relates the inputs $X(s)$ to the actuators to the outputs $Y(s)$ measured by the sensors. In the controller, the operator sets up the reference $Y_{REF}(s)$, the signal conditioning $F(s)$ (such as filtering when required), and the gain matrix transfer $G(s)$ whose function can be separated into three different terms as:

$$G(s) = (1 + \frac{1}{\tau_i.s} + \tau_d.s).C(s)$$

where $C(s)$ is the control gain matrix, and τ_i and τ_d the integral and derivative gains, respectively, also in matrix form.

In this process, the plasma transfer functions (or kernel) $K(s)$ is usually unknown, but can be identified either from power modulation experiments or by simulation using a predictive transport code such as CRONOS [41] or JETTO [42]. Real time profile control experiments have therefore motivated the activity on plasma transport modelling with the ultimate goal of reproducing the control experiments. Although full plasma transport modelling cannot yet fully replace the experiments for the design of controllers, they bring useful information on the dominant parameters for the design of a feedback control experiment. Once the plasma transfer function is identified, it is possible to simulate the control feedback loop and determine the most appropriate combination of controller gains (C, τ_i and τ_d) in $G(s)$ to ensure closed loop stability.

This layout does of course apply to the feedback control experiments with a single actuator and output. In the case of the control of β_N by NBI power presented in figure 4 for example, the kernel $K(s)$ has been modelled by a transfer function of the form:

$$K(s) = \beta_N(s)/P_{NBI}(s)=(0.116.s+0.57) / (0.29s+1).$$

From this model, the coefficients of G(s) can be determined either by trial and error simulation or using experimental techniques like the Ziegler-Nichols method [43]. In the case of this control experiment (figure 4), the control gains in G(s) are scalars and made of a proportional and integral term with $C = 8$, $\tau_i = 27$ (and $\tau_d = 0$).

3.2. EXPERIMENTAL DESIGN OF A CONTROLLER FOR THE REAL TIME CONTROL OF THE Q PROFILE.

For real time q profile control experiments with LHCD, NBI and ICRH powers as actuators, the general method is to build a linear Laplace response model around the target state to be controlled [12]. In this case the response matrix is built such that:

$$Q(s) = K(s) . P(s)$$

in Laplace form, where Q represents the safety factor difference vector and P the input power difference vector with respect to a reference discharge. Here, the kernel K(s) is determined experimentally using step or modulation experiments of the actuators. In this procedure each actuator is stepped up or down in three different pulses and the input power P and output Q differences are measured in their steady state limit after about one resistive time (i.e. for s=0). Figure 6 shows the step experiment in the case of the neutral beams. This experiment is performed on the same type of discharge as the long ITB discharge shown in figure 3. (B_T=3T, Ip=1.8MA, n=2.5. 10^{19} m^{-3}). After a few seconds, the real time q data are measured and the variation of q inferred for each of the five chosen control points (at r/a=0.2; 0.3; 0.4; 0.6; 0.8). This experiment is repeated for all three actuators. Singular value decomposition (SVD) expansion is performed on K(0) to identify the most significant singular values and to avoid over-determination:

$$K(0) = W(0) . \Sigma(0) . V^{+}(0) \tag{1}$$

As a result of SVD decomposition, $\Sigma(0)$ is a diagonal matrix. Matrix $\Sigma(0)$ is then truncated to the highest singular values, giving matrix $\tilde{\Sigma}(0)$ and providing the so-called steady state de-coupled modal input $\alpha(0)=V(0)^{+}.P(0)$ and output $\beta(0)=W(0)^{+}.Q(0)$ [12]. From this analysis, it is possible to invert the truncated diagonal matrix $\tilde{\Sigma}(0)$, and obtain a feedback control with a controller transfer function of the form from equation (1):

$$P(s) = G(s).(Q_{REF} - Q(s)) = V(0). \tilde{\Sigma}(0)\text{-}1. W(0)\text{+}. (1+\frac{1}{ô_i s}). Q_{REF} - Q(s))$$

Here, Q_{REF} is the q profile reference to achieve, τ_d=0 and τ_i is a constant chosen empirically but close to the typical current diffusion time.

It is important to note that this method has been generalised in reference 11 to include the control

of the pressure profile using the ρ^*_{Te} criterion as an input and also includes the use of appropriate basis functions for the output and input profiles (i.e. q and power deposition profiles).

3.3. EXPERIMENTS WITH REAL TIME CONTROL OF THE Q PROFILE.

As a proof of principle, this procedure has been first applied to the control of a pre-defined q profile of 5 points (r/a=0.2; 0.4; 0.5; 0.6; 0.8) with one actuator only, namely the LH power [44]. In this case the accessible targets are of course reduced to one family of profiles, so the reference points have been chosen close to the family inferred from the SVD analysis. The experiment is performed during an extended LHCD phase of 15s similar to those used to pre-form the q profile for the creation of an ITB ($Ip = 1.3MA$, $B_T = 3T$, $n = 2.510^{19}m^{-3}$). The Kernel K(s) is calculated from a simple LH power step experiment. The matrix K in this case has a size of [5x1] and Σ is reduced to a scalar and τ_i=1s. The real time q profile data are given by the Abel inversion of the polarimetric data as described in reference 21 and in section 2. Figure 7a shows the behaviour of the q profile traces together with their references and the LH power produced by the controller. The q profile reaches steady state and is maintained for about two resistive times. The LH-deposition profile (figure 7b) calculated by the ray-tracing code DELPHINE [45] included in CRONOS is consistent with the gains of the control matrix: i.e. the maximum deposited power corresponds to the maximum gain at r/a = 0.5. With this technique, reversed shear q profiles are also accessible and have also been achieved in steady state conditions by changing the reference value of the q profile [44].

After this first encouraging result, the SVD technique has been applied to the q profile control using three actuators (i.e. LHCD, NBI and ICRH). This time, the determination of the steady state plasma response is determined from one reference discharge and three dedicated step down experiments (one for each actuator) as explained in sub-section b. The Kernel K(0) is in this case a [5x3] matrix. Two out of three singular values ($\sigma_1 = 0.72$, $\sigma_2 = 0.22$, $\sigma_3 = 0.009$) have been retained by the SVD analysis in matrix Σ (indicating that the accessible q profiles are only a 2-parameter family [12]) and the integral time τ_i is still 1 second.

Figure 8a shows the resulting feedback waveforms together with the demand produced by the controller and the time traces of q at r/a = 0.5. Figure 8b illustrates the evolution of the q profile during the controlled phase (from 7 to 13s). Between 7s and 11s the q profiles falls sharply and then rises after 11s towards the reference points as the actuators start to act on the current density diffusion. This demonstrates that the selected gains were adequate and the technique effective on a time scale that approaches the current diffusion time scale [46]. Figure 9 shows the non-inductive current components generated by LH and the beams at 51s as calculated by JETTO. The separated deposition of these non-inductive currents (LHCD at mid-radius and NBCD in the plasma core) indicates that the q profile is controlled at two different radial points. This is consistent with the results from the above SVD analysis indicating that the accessible q profile targets are restricted to a two-parameter profile family. This successful experiment represents a step forward in view of a future application combining the q and pressure profile as an input in the controller.

3.4. SPACE-STATE METHOD MODELLING FOR THE OPTIMISATION OF THE CONTROLLER

In order to describe the dynamics of a system to be controlled, the state-space control method is often used in many areas since it has the advantage of handling more than one control input or more than one sensed output [43]. If P is the input to the system (NBI, ICRF and LHCD) and Q the outputs (including the q profile measurements at 11 radial locations, q_{95} and the loop voltage), the linear plasma response can be expressed as:

$$\frac{d\xi}{dt} = A.I + B.P \tag{2}$$

$$Q = H.\xi \tag{3}$$

where ξ is the state variable and A, B, H are matrices. Singular value decomposition is again used on Q to determine the principal components of the system and optimise the number of state variables ξ describing the system. A and B are then determined by classical system identification techniques. Figure 10 shows the modelling of the experiment described in the previous section. The SVD technique has determined that 4 state-space variables are sufficient to describe this system. The matrices A and B have been calculated from the step down experiments presented in the previous section. Knowing this model it is then possible to calculate the transient plasma response of the plasma using the Laplace transform on equation (2) and (3), leading to:

$$K(s) = \frac{Q(s)}{P(s)} = H.(s.I - A)^{-1}.B$$

where I is the identity matrix. The plasma response function (depending of s) is now represented in a linear form and can be used in a simulated control loop to determine the most appropriate PID gains (τ_i and τ_d) in G(s). This modelling is also a useful tool for the future design of controller for the simultaneous feedback of the q and pressure profile.

4. REAL TIME FEEDBACK CONTROL FOR PLASMA OPERATION

Real time feedback control tools have also been applied in JET to the operation of scenarios with regard to MHD instabilities and disruptions in particular. The active control of MHD modes deleterious to the confinement (such as NTMs) has already been achieved in JT-60 [7] and DIII-D [6]. Real time control has also been shown to be efficient for the control of resistive wall modes in DIII-D [6].

Figure 11 shows an example of an NTM controlled by power step downs in JET. This kind of experiment is not relying on the design of a PID controller but uses a simple event triggered by crossing a threshold level on the input MHD signal. In this case the root mean square signal of the n = 2 amplitude triggers a step down of the NBI and ICRH power as it exceeds a level of 0.1 volts corresponding to an island size of 6cm. When the NTMs induced by the sawtooth crashes reaches the

threshold level the additional power (NBI and ICRH) is stepped down. The same power level is re-applied when the n=2 signal goes back to zero i.e. when the NTM vanishes. The NTM reappears a second time before being completely stabilised at 17s. Note that the stored energy comes back to a higher level than before the NTM onset. At the end of this sequence, an m = 2 n = 1 NTM is destabilised and the power is stepped down thus preventing a likely disruption from occurring.

Disruptions are currently avoided at JET by the real time step down of the main heating when the pressure gradients become too steep, during an ITB scenario for example [48]. This is generally achieved using the neutron rate as an indicator of the limit of the pressure peaking and will be further developed using the new real time measurements. Another on-going effort is devoted to the classification of disruptions. A recent project aims to classify the disruptions in JET using the neural network technique [48]. This neural network is using plasma parameters as input (such as plasma current, internal inductance, radiated power, etc…) from the past four years of disruptions in JET. The results suggest that this technique can be ultimately used for the prediction and control of disruption [49], which will be an essential asset in a tokamak of the size of ITER.

Real time control also contributes to the operation of specific heating schemes and fuelling such as ^{3}He minority heating [13] and pellet injection [50]. An example of this is presented in reference [13] where the concentration of ^{3}He is being controlled in real time at a requested level to optimise the ICRH in a mode conversion experiment with ITBs. In this particular experiment the controller required a derivative term (i.e. $\tau_d \neq 0$) to account for the elapsed time between the opening of the valve and the penetration of the gas in the discharge which is of the order of 300-400ms in this case. The ^{3}He concentration has been controlled in a satisfactory manner even during the dynamic phases produced by the onset and vanishing of ITBs. This experiment could also be used as base for the control of the fuel mixes in future D-T plasma.

All these subjects are naturally highly relevant to the operation of the next step device and will certainly be further developed in JET to improve the safety and operation of the main plasma scenarios.

CONCLUSIONS

The recent development of real time measurements and control tools in JET has enhanced the integration of the relevant ITER scenarios. These new facilities are now used routinely in the JET experimental campaigns and offer to the scientific community a unique integrated set of real time diagnostics and processes for the control of plasma scenarios. In the past two years, challenging diagnostics such as the charge exchange diagnostic have been implemented in real time. Ambitious real time codes and processing such as the Grad-Shafranov solver EQUINOX have been successfully installed and validated. All these real time data are now strongly contributing to the reliability, reproducibility and protection of the plasma scenario in JET.

During the recent campaigns we have further developed three relevant scenarios for the next step device, namely the inductive scenario, the "hybrid" advanced tokamak scenario and the steady

state non-inductive scenario. Specific real time control networks have been developed for all three scenarios and have improved their reliability and reproducibility.

Real time control tools have been more specifically applied to the advanced tokamak scenario since they can assist efficiently in sustaining an internal transport barrier in a fully non-inductive plasma. For that reason specific model-base multi-variable techniques have been proposed for controlling the q and pressure profiles simultaneously. The JET experiments on q profile feedback control have validated these techniques and will provide a sound basis for future experiments to produce long (~20s) steady state discharges with $V_{loop} = 0$ using q and pressure profile control. Last but not least, the real time tools are also indispensable in preventing plasma instabilities developing such as neo-classical tearing modes or resistive wall modes. The real time control of the plasma fuel mix has also been achieved and this foresees future control of the D-T mix in a burning plasma experiment.

It is now demonstrated that real time measurements and control can play an increasing role in the integration of the scenarios relevant for ITER, and in the operation of a burning plasma experiment.

ACKNOWLEDGEMENTS

REFERENCES

[1]. Y. Shimomura et al., Plasma Phys. Control Fusion **43** (2001) A385

[2]. D. J. Campbell, Physics of Plasma, **8** (2001) 2041

[3]. D. Moreau and I. Voitsekhovitch, Nuc. Fus. **39** (1999) 685

[4]. A. Messian et al., Nuc. Fus. **34** (1996) 39

[5]. P. Gohil, Plasma Phys. Control Fusion **44** (2002) A37

[6]. E. J. Strait et al., Nuc. Fus. **43** (2003) 430

[7]. T. Ozeki et al., Plasma Phys. Control Fusion **45** (2003) 645

[8]. T. Wijnands, et al., Nus Fus **37** (1997) 777

[9]. A. Bécoulet et al., Plasma Phys. Control Fusion **43** (2001) A395

[10]. D. Mazon et al., Plasma Phys. Control Fusion **44** (2002) 1087

[11]. F. Crisanti, X. Litaudon, et al., Phys. Rev. Lett. **88** (2002) 145004

[12]. D. Moreau et al., Nucl. Fusion **43** (2003) 870

[13]. M. Mantsinen, et al., 2003 Plasma Phys. Control. Fusion, this issue

[14]. Becoulet A et al., Proceedings of the 15th Topical conference on radio frequency power in plasmas, AIP Conf. Proc. (2003), to appear.

[15]. R. C. Wolf et al, Plasma Phys. Control. Fusion **45** (2003) R1

[16]. F. Sartori, F. Cenedes and F. milani, Fusion Eng. Des. Vol 66-69 (2003) 735

[17]. O. Barana, E. Joffrin, A. Murari, and F. Sartori, Fusion Eng. Des. Vol 66-69 (2003) 697

[18]. Barana O., Murari A., Joffrin E., Sartori F. and contributors to the EFDA-JET workprogramme. Plasma Phys. Control. Fusion **44** (2002) 2271

[19]. P. Innocente, D. Mazon, E. Joffrin et al., Review of Scientific Instrument 74 (2003) 3645

[20]. L. Zabeo, et al., Proc. 30th EPS Conf. on Controlled Fusion and Plasma Physics (St Petersburg, 2003), Europhys. Conf. Abstract, (Geneva, EPS) P4.82.

[21]. L. Zabeo, A. Murari, E. Joffrin, et al., Plasma Phys. Control. Fusion **44** (2002)

[22]. M. Riva, L.Zabeo, E. Joffrin, et al., Fusion Eng.Des Vol 66-69 (2003) 779

[23]. J. Blum and H.Buvat, IMA Volumes in Mathematics and its Applications, Biegler & Coleman, **92,** part I, (1997) 17-36

[24]. K. Bosak, et al., Proc. 30th EPS Conf. on Controlled Fusion and Plasma Physics (St Petersburg, 2003), Europhys. Conf. Abstract, (Geneva, EPS), P3.164.

[25]. D. Mazon, et al., Proc. 30th EPS Conf. on Controlled Fusion and Plasma Physics (St Petersburg, 2003), Europhys. Conf. Abstract, (Geneva, EPS) ,O3.1C

[26]. N. Hawkes et al., Rev. Sci. Instrum. **70** (1999) 894

[27]. R. Gianella, et al., Proc. 30th EPS Conf. on Controlled Fusion and Plasma Physics (St Petersburg, 2003), Europhys. Conf. Abstract, (Geneva, EPS), P4.81.

[28]. M. Zerbini, J.M. Chareau, D. Mazon, M. Riva, R. Felton, E. Joffrin, M. Lennholm, R. Prentice. Fast ECE Diagnostics Applications For Real Time Control at JET. Proceedings of 12th Joint Workshop on ECE and ECRH, Aix-en-Provence (France) May 2002; ed. by G. Giruzzi, World Scientific, p. 227.

[29]. M. Riva et al., Proc. 19th IEEE/NPSS Symp. on Fusion Eng. 2002 (Atlantic City, USA).

[30]. P. Heesterman et al., Rev. Sci. Instrum. **74**, (2003) 1783.

[31]. G. Tresset, et al., Nus Fus **42** (2002) 520

[32]. R Barnsley et al., Rev. Sci. Instrum. **74**, (2003) 1969

[33]. R.Felton, K.Blackler, S.Dorling, et al., IEEE Transactions on Nuclear Science, **47** (2000) 174

[34]. J. Ongena et al., Plasma Phys. Control. Fusion **43** (2001) A11

[35]. P. Dumortier, et al., Proc. 30th EPS Conf. on Controlled Fusion and Plasma Physics (St Petersburg, 2003), Europhys. Conf. Abstract, (Geneva, EPS), P1.91.

[36]. V. Pericoli-Ridolfini, et al., Proc. 30th EPS Conf. on Controlled Fusion and Plasma Physics (St Petersburg, 2003), Europhys. Conf. Abstract, (Geneva, EPS), P4.89.

[37]. E. Joffrin et al., Nuclear Fusion, volume 43, (2003), 1167

[38]. A. C. C. Sips et al., Control. Fusion **44** (2002) B69

[39]. A.C.C Sips, et al., Proc. 30th EPS Conf. on Controlled Fusion and Plasma Physics (St Petersburg, 2003), Europhys. Conf. Abstract, (Geneva, EPS), O1.3A.

[40]. S. Pinches et al., "MHD in Advanced Scenarios", this conference.

[41]. V. Basiuk, et al, Nuclear Fusion, vol. 43 (2003) 822

[42]. 'Genacchi G and Taroni A, "JETTO: A free boundary plasma transport code (basic version)", Rapporto ENEA RT/TIB 1988(5)'.

[43]. G. F. Franklin and J. D. Powell, "Feedback control of dynamic systems", Addison-Wesley Publishing Company, third edition, (1995).

[44]. D. Mazon et al., Plasma Phys. Control Fusion **45** (2003) L47

[45]. F. Imbeaux, Report EUR-CEA-FC number 1679, (1999).

[46]. F. Crisanti, et al., Proc. 30th EPS Conf. on Controlled Fusion and Plasma Physics (St Petersburg, 2003), Europhys. Conf. Abstract, (Geneva, EPS), P2.88

[47]. G.T.A. Huysmans et al., Nuc. Fus. **39** (1999) 1489-1507

[48]. M.K. Zedda, et al., Proc. 30th EPS Conf. on Controlled Fusion and Plasma Physics (St Petersburg, 2003), Europhys. Conf. Abstract, (Geneva, EPS), P2.93.

[49]. G. Pautasso et al., Nuc. Fus. **42** (2002) 100

[50]. P. Lang et al., Nucl. Fusion **42** (2002) 388-402

Real time diagnostic	Real time data produced	Source data sampling
Magnetics	MHD (n=1 and n=2)	2ms
Interferometer	Fringe jump corrected line integrated density	2ms
polarimeter	Faraday angles	2ms
Motional Stark Effect	Pitch angles	2ms
Charge exchange	$T_i(R)$, and toroidal rotation (11 channels)	50ms
ECE	$T_e(R)$ on 96 channels	2ms
Visible spectrometry	D_α signal, He^3, T, H	2ms
	Fe, Ni, lines etc …	15ms
Crystal spectrometer	Ar, N, Fe, Ni, etc…lines	2ms
Bolometry	Radiation lines of sight	2ms

Table I: Real time diagnostic implemented in JET

Real time processes	Real time diagnostic inputs	Real time data produced	Source data sampling
Confinement	Magnetics, Additional heating power	W_{dia}, τ_E, β_N, li, etc..	2ms
Equilibrium (EQUINOX)	Magnetics, interferometry, polarimetry	Plasma shape and flux surface geometry, q and density profile	20ms
Profile mapping	T_e, T_i, n_e, pitch angles, faraday angles faraday angles	T_e, T_i, and q profiles, thermal energy, ITB criterion [32], etc…	20ms
ELMs	D_α line	Frequency and growth rate of ELMs	2ms

Table II: Real time processes implemented in JET
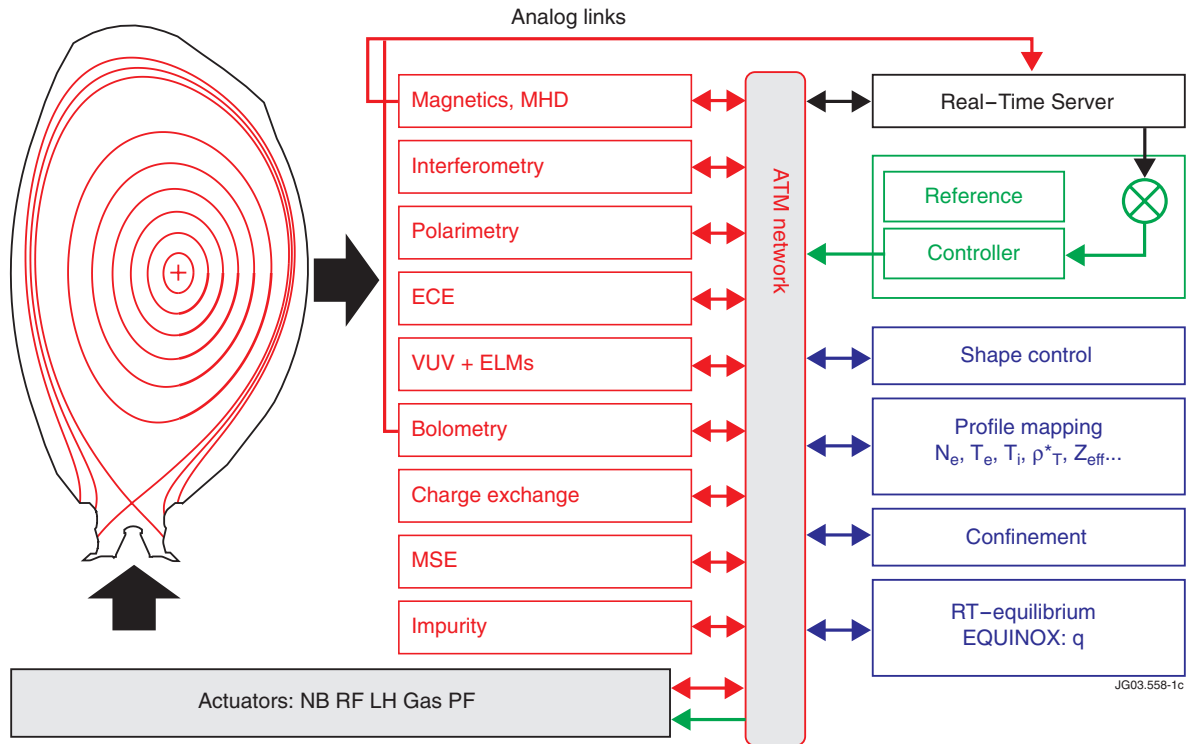
Figure 1: Real time measurement and control system developed at JET. This system comprises real time diagnostic (left, see table I), the real time processes (bottom right, see table II), and the real time signal server and central controller (top right) where the gains are set up for a feedback control experiment. All these systems are connected to the ATM (Asynchronous Transfer Mode) communication network.
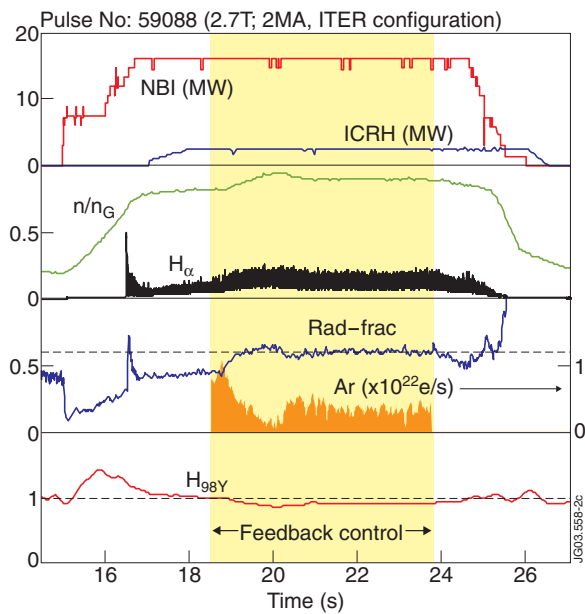

Figure 2: Typical inductive scenario operated at JET with an ITER-like magnetic configuration with NBI. Here (third box from top), the radiation fraction is controlled at 60% (dotted line) in real time by the argon injection. The confinement is not degraded significantly (box 4) by the impurity injection. This discharge has high frequency type I ELMs (~50Hz) and is operated at 85% of the Greenwald density (box 2).
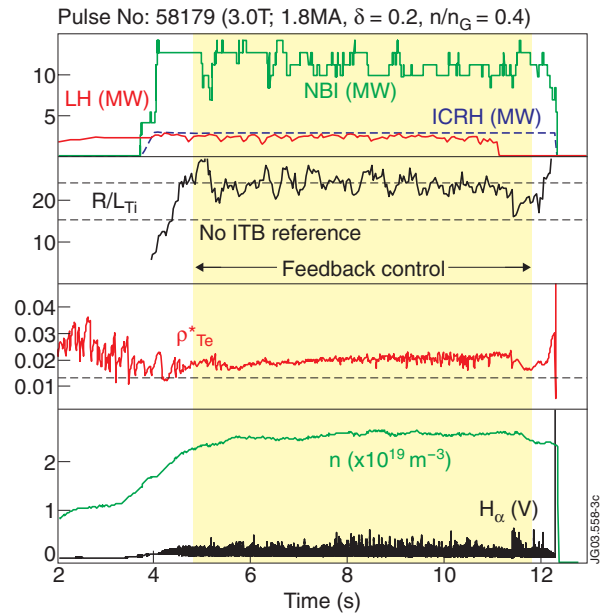
Figure 3: Steady state scenario with controlled transport barrier in JET with NBI (plain line), LHCD (dotted line) and ICRH (dashed) power. The ITB lasts for 8s and is controlled (second box from top) by the neutral beam using the parameter R/L_{Ti} set to 24 as reference. The ρ^*_{Te} parameter (box 3) is also very steady at a value of about 0.02 above the ITB existence criterion [29] threshold of 0.014.
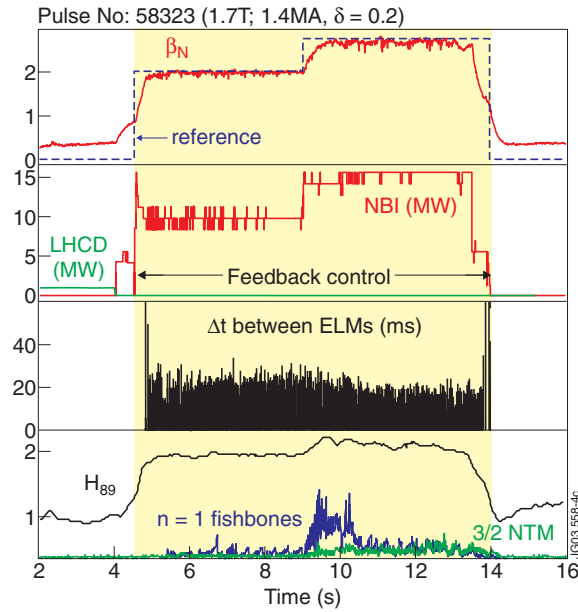
15

Figure 4: Example of the "hybrid" advanced scenario in JET. The β_N is controlled in real time by the neutral beam power and reaches 2.8 (first box from top). H_{89} exceeds 2.1 and does not seem to be affected by the onset of low amplitude neo-classical tearing modes (box 4). The time delay between ELMs (box 3) is calculated by the real time detector and confirms the high frequency (~40Hz) of type I ELMS in this regime.
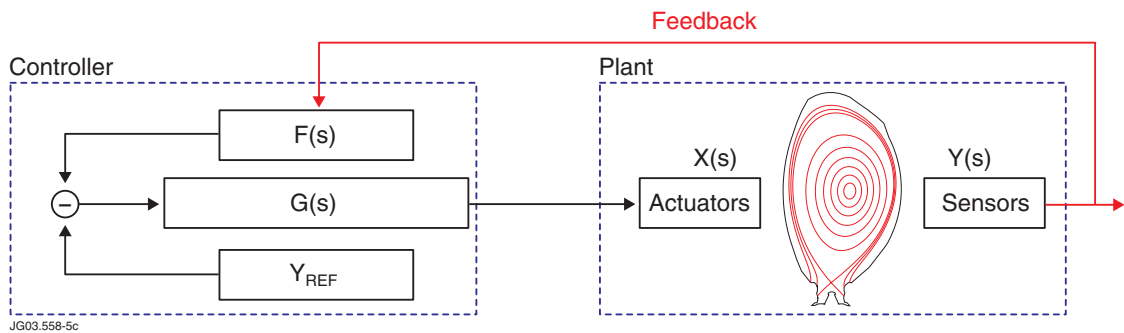

Figure 5: Schematic layout of the system for control feedback experiments in a tokamak. In the plant, the plasma transfer function K(s) relates the inputs X(s) to the actuators to the outputs Y(s) measured by the sensors. In the controller, the operator sets up the reference YREF(s), the signal conditioning F(s) (such as filtering), and the gain matrix transfer G(s).
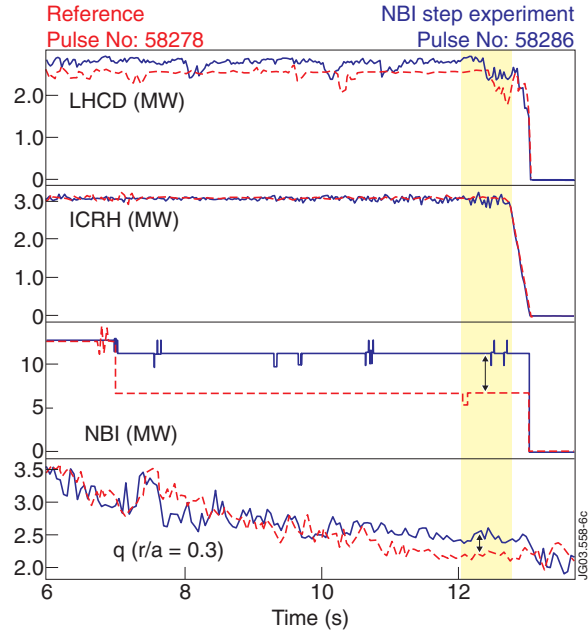
Figure 6: Typical step-down experiment used for the determination of the control matrix. In this example, the NBI power is stepped down (dashed lines, third box) with respect to the reference pulse (plain line) the δp input and the output δq differences are measured (double arrows) in their steady state limit (i.e. for s=0) after about one resistive time in the shaded window indicated between 12 and 13s. This experiment is then repeated for the two actuators (ICRH and LHCD) to complete the determination of the K(0) matrix.
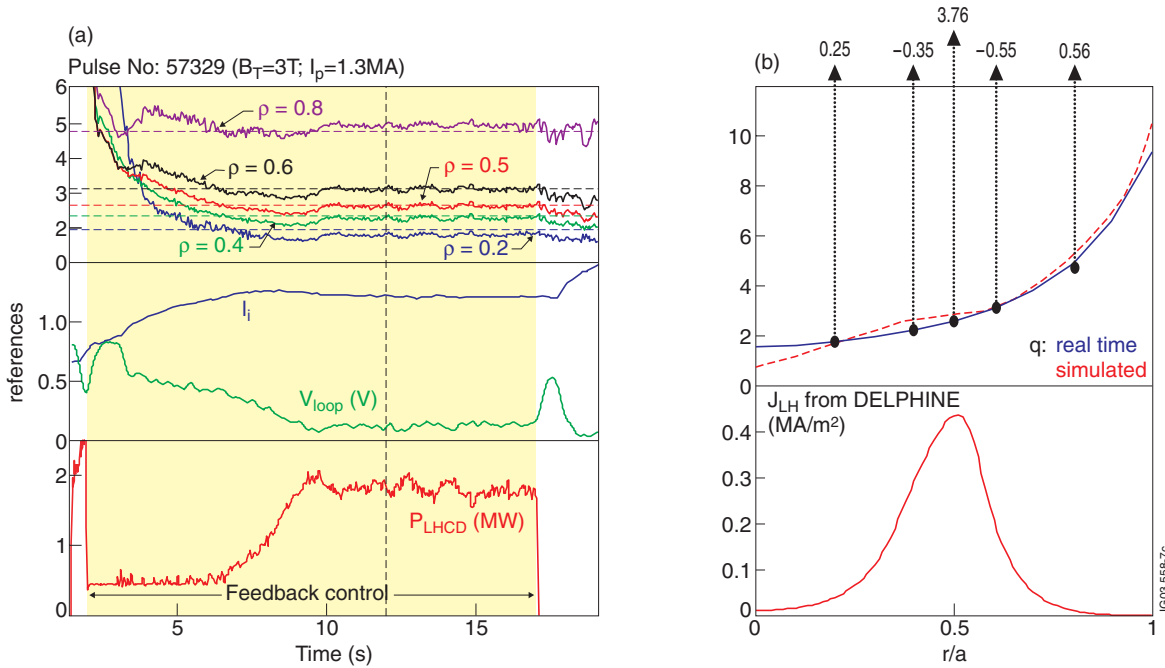
Figure 7(a): Real time control of the q profile with LHCD only. On the top, the safety factor time traces are compared with the q reference used in the controller. In the centre, the internal inductance (li) and loop voltage (V_{loop}) are demonstrating that this discharge reaches steady state.

Figure 7(b): Comparison of the q profile measured from real time data and the simulation from the CRONOS code (dotted line) at 12s (indicated by the dotted line on figure 7a). The five filled circles show the reference q values used in this experiment. The gains of the control matrix are displayed on the top of the graph. The highest gain (3.76 at r/a=0.5) is consistent with the location of the maximum
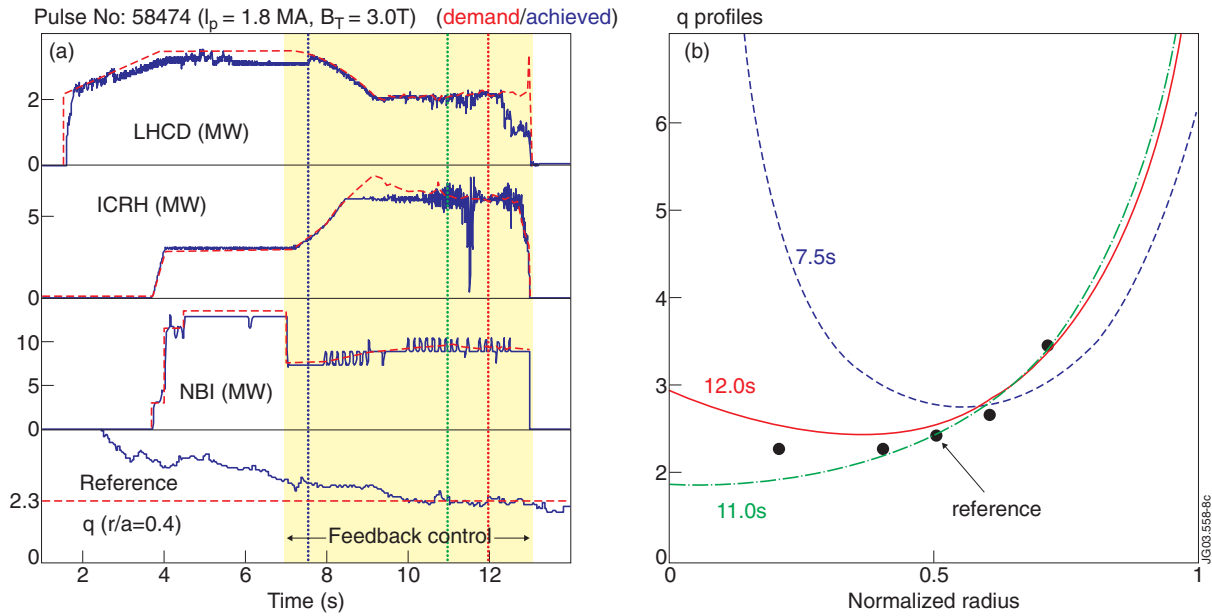
17

Figure 8(a): Real time control of the q profile with three actuators (LHCD, ICRH, NBI). The power demanded by the controller (dashed lines) are compared with the delivered power from the heating systems in the three top graphs. Between t=8.5s and 10s, the ICRH could not deliver the demanded power due limitation of the pre-programmed maximum power at 6MW. However after t=10s, the demand comes back down to the delivered level. The q(t) at r/a=0.4 (bottom trace) reaches its reference value at 10s and keeps around it for about 3s.

Figure 8(b): q profile evolution at 7.5, 11 and 12s during the control phase of pulse 58474. The filled circles also indicate the reference values. The q profile reaches the references at 12s after about one resistive time.
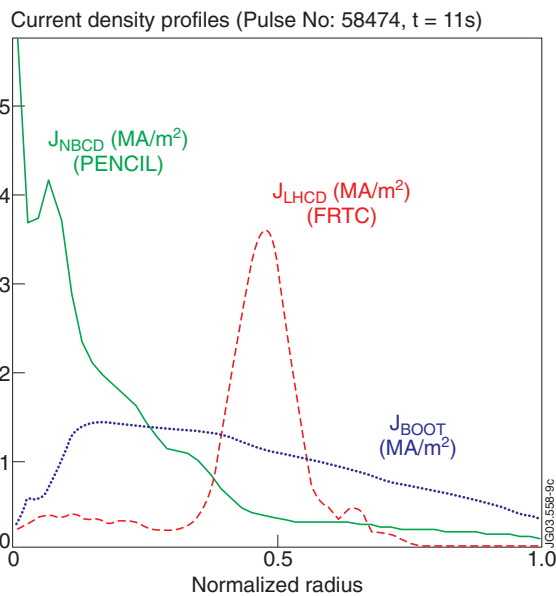

Figure 9: Non-inductive current components from the JETTO simulation of the pulse presented in figure 8a and 8b at 11s. Beam current (plain line), LH-driven current (dashed), bootstrap current (dotted).
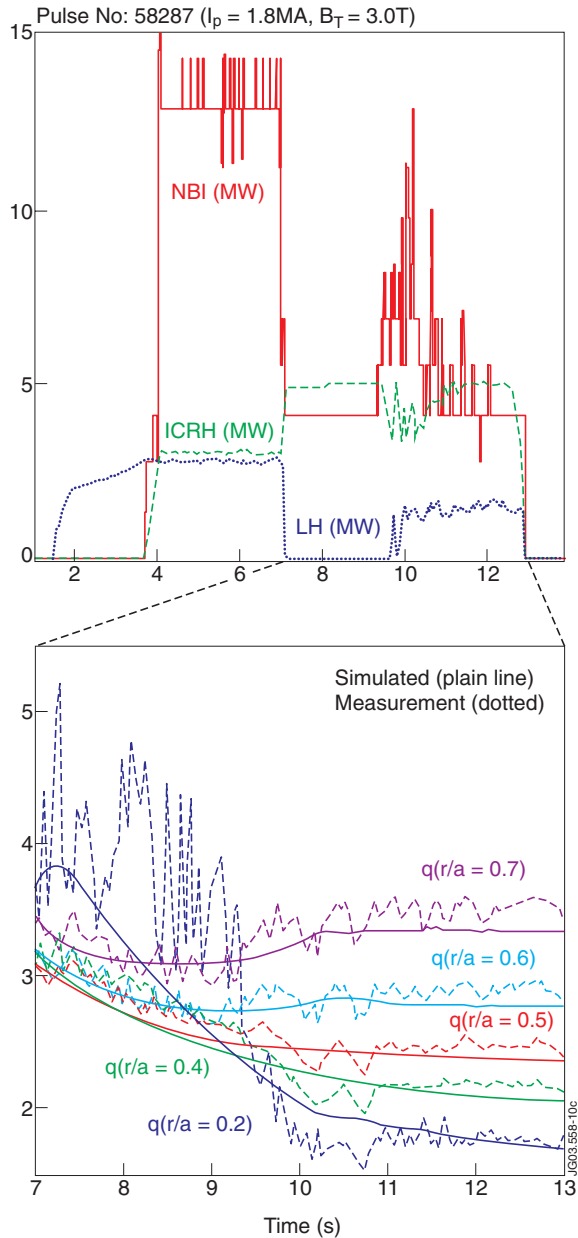
18

Figure 10: Modelling of the q profile of a discharge heated by LHCD (dotted), ICRH (dashed), and NBI using the space-state method. The model has been computed using experimental data from the step-down power experiment such as that of figure 6. The bottom graph shows good agreement between the simulated data (plain line) and the experimental data (dashed) during the transient phase of the discharge at five different radial locations.
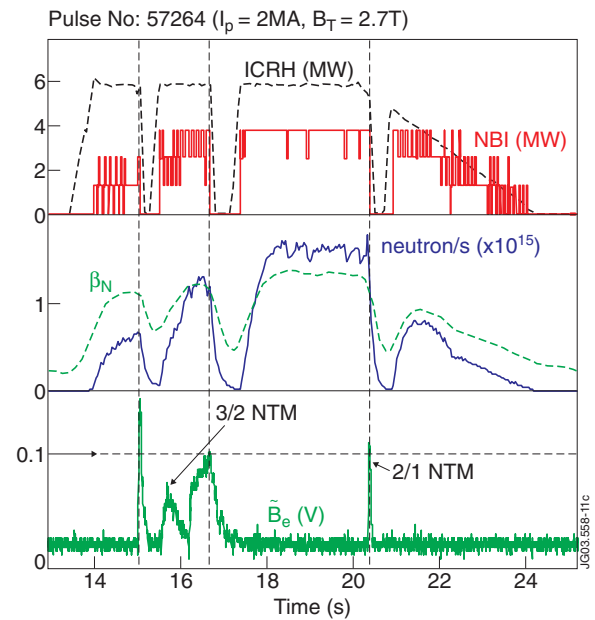
Figure 11: Active control of neo-classical tearing modes (NTM) by event driven power steps down. When the n=2 mode amplitude (bottom box) exceeds a threshold value of 0.1Volt (corresponding to an island size of about 6cm), the NBI and ICRH (dashed) power are stepped down (top box) till the mode decays below another low threshold value. After the first event at 15s, β_N (dashed) is not reduced sufficiently and the NTM re-strikes when the power is re-applied. The second power reduction does completely stabilise the NTM and β_N goes up to a higher value than before the NTM occurrence. At 20s, an m=2 n=1 NTM grows producing another step down of the power which prevents a likely disruption to occur.